European Journal of Pharmaceutics and Biopharmaceutics 212 (2025) 114736

Contents lists available at ScienceDirect

European Journal of Pharmaceutics and Biopharmaceutics

journal homepage: www.elsevier.com/locate/ejpb

Research paper

# Flexipill: A novel 3D printed flexible dose combination for hypertension with a floating element

Yasir Karkar [a], Tanzeela Anis [b], Amal Ali Elkordy [a], Ahmed Faheem [a,c,*]

[a] School of Pharmacy and Pharmaceutical Sciences, University of Sunderland, Sunderland SR1 3SD, United Kingdom
[b] Faculty of Science, Agriculture and Engineering (SAgE), Newcastle University, Newcastle NE1 7RU, United Kingdom
[c] RAK Medical and Health Sciences University, Ras Al Khaimah, United Arab Emirates

ARTICLE INFO

*Keywords:*
3D printing
Fused deposition modelling
Personalised medicine
Polypill
Floating tablet
Hypertension

ABSTRACT

Hypertension is highly prevalent worldwide, affecting approximately one in three adults. The pathophysiology of hypertension is multifactorial, which led recent guidelines to recommend the initiation of treatment with more than one antihypertensive agent. This exacerbates the existing issue of polypharmacy, particularly among geriatric patients. Polypharmacy can lead to a reduction in patient adherence to the treatment. As a result, many clinical studies have investigated using fixed-dose combinations to address this issue. These studies have demonstrated the effectiveness of a polypill in improving patient adherence. However, a polypill limits the flexibility for dose titration and personalisation of treatment. Therefore, when 3D printing was first introduced to pharmaceutical formulation, researchers recognised the potential of this technology for drug personalisation and the creation of more flexible drug combinations. Nonetheless, regulatory concerns still limit the translation of these research efforts into clinical applications that can benefit the patient. Consequently, this study seeks to bridge the existing gap by identifying a balanced approach between regulatory requirements and the concept of personalised drug combinations.

The Flexipill is a flexible dose combination that does not require printing at the pharmacy level. It can be printed at a quality-controlled facility and assembled according to patient needs at the point of care. In this work, an antihypertensive Flexipill was printed, with each unit having different drug release profiles and formulation requirements. The propranolol HCl unit was printed as a floating unit to improve its solubility and bioavailability. It floated for 9 h, releasing over 90 % of the drug content. The enalapril maleate unit was formulated to avoid thermal degradation by printing at 150 °C, which is lower than its degradation temperature. Moreover, hydrochlorothiazide was formulated to provide immediate release of over 90 % of the drug within the first hour.

## 1. Introduction

Hypertension is one of the significant risk factors for cardiovascular diseases (CV) and renal disease, affecting 25 % of the population [1]. Although, most clinical hypertension researches reflect the effect of antihypertension therapy in reducing CV events [2]. Nonetheless, many studies reported that less than 50 % of patients reach their systolic blood pressure goals [3–5]. This lack of control is often attributed to practitioners avoiding aggressive therapeutic strategies to manage hypertension [2]. However, other reviews suggest that systolic blood pressure control remains challenging, even in clinical trials where patient compliance and physician expertise are ensured [6]. Consequently, the recent guidelines recommendation was to start treatment with a combined antihypertensive agent [7,8].

Additionally, the data available suggest that more than 70 % of the patients with hypertension will eventually require at least two antihypertensive agents [9–11]. Hypertension has a multifactorial pathophysiology; combining more than one agent increases efficacy and decreases side effects [2]. Nevertheless, polypharmacy, especially in geriatric patients, can lead to a reduction in adherence to the treatment and eventually its failure [5,12]. Therefore, a bulk of research has directed attention towards fixed-dose combinations (FDC) or polypills as the solution to improve adherence and reduce the cost of polypharmacy [13–15]. An FDC is a single dosage form that contains more than one

* Corresponding author at: School of Pharmacy and Pharmaceutical Sciences, Faculty of Health Sciences and Wellbeing, University of Sunderland, Sunderland SR1 3SD, United Kingdom.
*E-mail address:* ahmed.faheem@sunderland.ac.uk (A. Faheem).

https://doi.org/10.1016/j.ejpb.2025.114736
Received 24 November 2024; Received in revised form 22 April 2025; Accepted 6 May 2025
Available online 8 May 2025

API, and it can be delivered as a capsule, injectable or tablet (polypill).

Nevertheless, FDCs have many concerns, such as the difficulty of titration of one of the components, difficulties in treatment discontinuation, possible physical and chemical interaction between the different APIs and different solubility pharmacokinetics, which leads to differences in formulation requirements for each component [16]. However, in recent years, the advancements in 3D printing have encouraged many researchers to investigate the use of this technology to print polypills that can be customised according to patient needs at the point of care [17–20]. Pharmaceutical research has introduced several technologies, but fused filament fabrication remains the most studied due to its simplicity and cost-effectiveness [21].

However, 3D printing of personalised pharmaceutical products at the point of care raises many regulatory concerns [22]. The current practice is to regulate personalised 3D-printed medication through guidance for extemporaneous preparation [23]. Nonetheless, this can only be done on a small scale. Consequently, to address the significant challenge of hypertension control, a personalised polypill that can be prepared and regulated within the framework of a large-scale industry is needed.

In this work, using fused filament fabrication (FFF), an attempt was made to formulate units that can be 3D printed and tested in a manufacturing site and thereafter can be personalised according to patient needs by assembling at the point of care into a polypill (FlexiPill). The design was composed of multiple frustums that can be stacked on top of each other. Three antihypertensive medications were used as the model APIs: propranolol, enalapril and hydrochlorothiazide. In addition to the synergistic benefit to hypertension of using more than a single agent, ACE inhibitors decrease the diabetogenic risk compared to monotherapy with HCT or Propranolol alone [24].

Each of these antihypertensive drugs has different formulation requirements. Propranolol has higher solubility in the acidic medium of the stomach and is subject to degradation in the alkaline medium of the small intestine [25]. Therefore, propranolol bioavailability can be improved if formulated in gastroretentive formulation. Floating tablets are one of the well-known strategies for gastric retention. It has been demonstrated in previous research that FFF can offer a significant advantage in formulating floating tablets with no lag time compared to the old traditional formulation technique of floating tablets [26,27].

On the other hand, enalapril is a thermolabile drug that degrades at a temperature of 160 °C [28], making processing with FFF challenging. Finally, Hydrochlorothiazide is a class II drug according to the BCS with low solubility and good permeability. Hence, its bioavailability can be improved if formulated into a solid dispersion in a hydrophilic polymer [29].

The objectives of this study are twofold: First, fabricate the Flexipill design and demonstrate its efficacy in delivering drug combinations inflexibly, enabling personalised therapy. Second, it meets the specific formulation needs of each active pharmaceutical ingredient (API): gastric retention for propranolol, thermal stability for enalapril, and immediate release for hydrochlorothiazide.

## 2. Materials and methods

### 2.1. Materials

Propranolol (PR) was purchased from Thermo Fisher Scientific (Waltham, MA, USA). Enalapril maleate (EM) and hydrochlorothiazide (HCT) were purchased from Molekula Ltd (Darlington, UK). Triethyl citrate (TEC), Talc, Polyethylene oxide 200,000 g/mole (PEO), polyethylene glycol 4000 g/mole (PEG 4000) and polyethylene glycol 6000 g/mole (PEG 6000) were purchased from Sigma-Aldrich Ltd (UK). Eudragit EPO (E EPO) and Eudragit RLPO (E RLPO) were provided as a donation from Evonik Industries (Darmstadt, Germany). Scotch blue painter's tape 50 mm was supplied by 3 M (Bracknell, UK).

### 2.2. Methods

#### 2.2.1. Filament preparation

Formulations were mixed with glass mortar and pestle for 5–10 min, then fed through the hopper of a single screw extruder (Noztec Pro hot melt extruder, Noztec, Shoreham-by-Sea, UK) to be extruded into filaments. The nozzle diameter was 1.75 mm and the screw speed was 15 rpm. The filament was printed directly after extrusion to decrease the effect of humidity.

#### 2.2.2. Design and printing

Designing the frustums of the Flexipill was done using Autodesk® Tinkercad™ free online software (Autodesk, CA, USA). Two types of frustums were designed, both measuring 5 mm in height with a 3.75 mm base radius and a 2.5 mm top radius. One featured a closed base to enclose the central space, while the other had an open base to allow access to the central cavity, facilitating the connection between units. Thereafter, the.stl file was exported for the slicing software of MakerBot Replicator + (Makerbot Industries, LLC., USA) to be printed. The printer contain one print head with nozzle diameter of 0.6 mm, with a printing speed of 40 mm/ second and a first layer thickness of 0.8 mm. The print was then extruded into a heated building platform system from (IDE Vesterling, Germany) covered with blue scotch tape to improve adhesion.

#### 2.2.3. Rheology

Complex viscosity was measured using a Kinexus rheometer from Malvern (Malvern Instruments, Worcestershire, UK) with 25 mm/ 65 mm upper/lower smooth parallel plates. The formulations were pressed to a 25 mm disc after extrusion and 1 mm thickness. Thereafter, a frequency sweep was performed from 100 to 0.1 Hz and 1 % shear strain. The temperature was set to 150 °C during screening, while the printing temperature for each formulation was used to evaluate the viscosity at the print.

#### 2.2.4. Scanning electron microscope

A scanning electron microscope (SEM) (Hitachi S300N electron microscope, Hitachi, UK) was used to examine the surface morphology of tablets and filaments and the uniformity of the printed layer. The samples were placed on aluminium stubs 25 mm in diameter with carbon double adhesive. Then, they were coated with a gold–palladium coat in an Argon atmosphere at about 10 Pa for 1 min to improve conductivity and image resolution. The scanning electron microscope was set to 20 Kv.

#### 2.2.5. Thermal analysis

Thermal gravimetric analysis was conducted using a METTLER Thermal Analyzer (Mettler Instrumente AG, Greifensee, Zurich). The Sample was placed in 100 μl aluminium pans, and the temperature was ramped from 25 °C to 600 °C with a heating rate of 10 °C /minute.

Thermal analysis was performed using differential scanning calorimetry (DSC) with (TA instruments Q1000) and hermetic aluminium pans. Heat/cool/heat circle was performed at 10 °C/min heating and cooling rates, and the temperature was lowered to zero until equilibrium was reached before the start of the experiment. The highest temperature was decided depending on the initial degradation temperature measured in TGA. The nitrogen purge rate was set at 50 ml/min, and the sample weight was in the range of 5–10 mg.

#### 2.2.6. Fourier transform infrared spectroscopy (FTIR)

FTIT Spectrum for the APIs and tablet units was measured and analysed using an FTIR Spectrophotometer (Perkin–Elmer, Cambridge, UK). The frequency range used was 4000–550 $cm^{-1}$ at 2 $cm^{-1}$ resolution, and the number of scans was 32. Happ-Genzel was used as an apodization function.

#### 2.2.7. Powder X-ray diffraction (PXRD)

The diffraction pattern needed to be taken to determine the API's crystallinity in the final printed product. Samples were printed onto 25 mm discs, and the pure APIs and physical mixtures of the powder formulations were used as controls. The sample was mounted into the sample holder using Putty, and the control powder was placed in a 16 mm sample holder.

An X'Pert-MPD PANalytical X-ray diffractometer (X'PertMPD, PANalytical, The Netherlands) was used with soller slit = 0.02 rad, Ni Kβ filter, 2θ range: 5–30°, step size = 0.0334°, scan speed = 0.03°/s.

#### 2.2.8. Drug content and dissolution test

Frustum units were milled using a mortar and pestle to measure the drug content within the units. A finite amount of the milled units was then weighed. 83.3 mg, 100 mg, and 120 mg of propranolol, enalapril, and hydrochlorothiazide units, which are equivalent to 25, 15 and 15 mg of propranolol, enalapril, and hydrochlorothiazide. Afterwards, the milled powders were dissolved in 250 ml of methanol respectively. Then, 2 ml was transferred to HPLC vials and measured using the method described in the next section.

The dissolution test was performed using USP apparatus 2 with rotating paddles. The rotation speed was set at 100 rpm, the temperature was set at 37 ± 0.5 °C, and the dissolution medium was 1000 mL of 0.1 M Hydrochloric acid (HCl)at a pH of 1.5. Samples were collected using 10 ml syringes at 10, 20, 30, 60, 120, 240, 360, 540, 720, and 1440 min using 10 mL syringes and filtered using 0.2 μm PTFE syringe filters into 2 mL tented HPLC vials.

#### 2.2.9. Chromatographical analysis

High-performance liquid chromatography (HPLC) was employed to quantitatively determine the amount of each active pharmaceutical ingredient (API) in the drug content analysis and the dissolution test after all the samples from all the dissolution vessels were collected. The HPLC system was an Agilent 1290 infinity HPLC system coupled with a G4212A diode array detector (DAD) (Agilent Technologies, Inc., Santa Rosa, CA). The stationary phase was a reversed phase Luna 3 μm Phenyl-Hexyl (100x4.6 mm) column. The mobile phase was a gradient mixture of D.W. containing 0.1 % phosphoric acid (solution A) and methanol (solution B). Table 1 presents the gradient mixture of the aqueous and organic solutions. The flow rate was 0.4 mL/min. The detection wavelength was set to 210 and 280 nm, and the run time was 15 min. Three calibration graphs for each APIs were constructed with 21 points and used to calculate the amount of the drugs in the drug content and dissolution experiments. The ranges for propranolol and enalapril calibration curves were between 6 and 50 mg, while the calibration curve for hydrochlorothiazide was between 1 and 25 mg. The same method was used for liquid chromatography-mass spectrometer (LC-MS) with one change: the phosphoric acid in the aqueous part of the mobile phase (solution A) to formic acid. Agilent single quad detector (Agilent Technologies, Inc., Santa Rosa, CA) was used.

#### 2.2.10. Kinetic model fitting

Microsoft Excel was used to solve for the least Residual Sum of Squares (RSS) between the prediction model and the release data to fit the three drugs' release to a kinetic model. The data point used was before reaching plateau. Afterwards, the correlation coefficient ($R^2$) between the prediction and release data was calculated.

Thereafter, the Akaike Information Criterion (AIC) were computed for each model using the RSS, with the equation:

$AIC = n \ln(RSS/n) + 2k$ [30]

Where n is the number of data points used, K is the number of model parameters and RSS is the Residual Sum of Squares.

**Table 1**
The gradient method for eluting the mobile phase in the HPLC method.

| Time (minutes) | Methanol (organic phase) | D.W./0.1 % phosphoric acid (aqueous phase) |
|---|---|---|
| 0–3 | 20 % | 80 % |
| 10 | 55 % | 45 % |
| 10.1 | 20 % | 80 % |
| 15 | 20 % | 80 % |

## 3. Results and discussion

### 3.1. Design and formulation

This work addressed two types of challenges: a design challenge and a formulation challenge. The design challenge involved creating a flexible dosage combination that could be easily assembled according to patient-specific needs while maintaining the overall size within acceptable limits and incorporating a functional floating unit. Compounding using 3D printing technology has gained interest in recent years due to its ability to automate the compounding process to produce personalised dosage forms. However, this has been raising regulatory concerns regarding the quality and safety of the final product [31,32]. The Flexipill design enables the flexibility to tailor the polypill's components and dosage directly at the point of care using pre-printed, quality-controlled units that can be assembled at the point of care, removing the need for on-site printing. Each unit will contain one API to provide flexibility to that the conventional polypill lack, by adding or removing medication on demand. This approach can help address regulatory concerns related to the quality and safety of the final product while also enabling broader personalisation, ultimately benefiting a more significant number of patients than is currently possible. Secondly, a formulation challenge unique to each API will be discussed in detail later. From a design perspective, the Flexipill with the staked frustums is designed in such a way that 2 mm of the bottom frustum goes inside the top one, leaving 3 mm. As a result, each additional unit will add 3 mm to the total length of the Flexipill after the initial 5 mm of the first frustum. Hence, even a Flexipill with five units will have a length of less than 2 cm and a diameter of 7.5 mm, which is smaller than a size 0 capsule, making it easily swallowable. Patient compliance can be further improved by containing the Flexipill in a capsule or adjusting the design in the future to have smoother sides.

Additionally, to ensure that the propranolol unit (PR-U) will float in the gastric juice, its density must be lower than that of the gastric fluid. Therefore, the PR frustum was designed to have a closed base with a hollow centre, while the other units are intended to sink after detachment from it. The volume must be calculated to calculate the density of each frustum, and then the weight of each frustum must be divided by its volume.

From the formulation perspective, the floating frustum must release the API by means of diffusion with no polymer erosion since any erosion to the walls of the units can lead to the entry of the dissolution medium into the hollow centre, which can result in the sinking of the unit. Hence, the PR unit was formulated with Eudragit RLPO (E RLPO) as the primary polymer because of its pH-independent release of the API through swelling of the polymer and diffusion of the dissolution media [33]. An additional contingency was drug load, which must be relatively high to achieve a 40 mg dose per unit. This led to a unit with 155.4 $cm^3$ volume and a mean weight of 147.6 ± 2.1 mg. As a result, the unit density was 0.95 $cm^3/g$, which is lower than the gastric fluid density of 1.003 $cm^3/g$, resulting in the flotation of the unit [25]. Table 2 presents the frustums' mean weight, mean drug content, calculated volume and calculated density.

On the other hand, EM-U and HCT-U should have immediate release formulations with erosion of the units to disconnect from the PR floating unit. As a result, Eudragit EPO (E EPO), a cationic methacrylate polymer, was chosen as the primary polymer to print these units since its immediate release of the API in the acidic medium has been established [34]. Additionally, enalapril has an additional challenge due to its

**Table 2**
Frustum units' weight, drug content, volume and density.

| | Mean unit weight | API dose | Drug content | Volume | Density |
|---|---|---|---|---|---|
| **EM-U*** | 136.9 ± 1 mg | 20.54 ± 0.15 mg | 102.88 ± 1.24 % | 93 $mm^3$ | 1.47 g/$cm^3$ |
| **HCT-U**** | 111.1 ± 3.8 mg | 13.88 ± 0.47 mg | 97.59 ± 4.21 % | 93 $mm^3$ | 1.19 g/$cm^3$ |
| **PR-U***** | 147.6 ± 2.1 mg | 44.28 ± 0.63 mg | 96.23 ± 3.05 % | 155.4 $mm^3$ | 0.95 g/$cm^3$ |

* EM-U = enalapril maleate unit, **HCT-U = hydrochlorothiazide unit, ***PR-U = propranolol unit.

thermolabile nature, making the drug liable to degradation at the high temperature of the HME and FFF. Consequently, the enalapril formulation needs to be extruded and printed at low temperatures. Although E EPO has a Low Tg of 48 °C [33] and can be processed at a low temperature, filaments produced with E EPO are brittle, and multiple strategies have been suggested to improve its printability [35,36]. One of these effective strategies was the addition of a high molecular weight polymer as a flexibility modifier to improve its printability and decrease its brittleness. However, adding the high molecular weight polymer can increase the melt's viscosity, leading to a higher printing temperature. The effectiveness of this strategy was demonstrated by Than et. al, who used Hydroxypropyl cellulose-L (HPC-L) with a molecular weight of 140,000 g/mole as the flexibility modifier and the printing temperature had to be raised to 200 °C [37].

Additionally, a different research group used polyethylene oxide (PEO) with a molecular weight of 100,000 g/mole to improve the flexibility of E EPO. Still, the filament had to be printed at 190 °C [28]. Nonetheless, Alhijjaj et. al also used PEO 100 K and managed to decrease the printing temperature to 150 °C by adding polyethylene glycol (PEG) 4000, which was used to adjust the viscosity of the formulation [38]. Therefore, in this work, PEO 200,000 g/mol was used as a flexibility modifier to improve filament printability but at low concertation and with the use of PEG 6000 as a viscosity modifier for the polymer blend and, consequently, the printing temperature.

### 3.2. Enalapril formulation screening

The screening was performed to determine the best percentage of PEO to E EPO. Thereafter, the complex viscosity of the polymer mix was measured, and the printability was evaluated using the printer. Talc was used for screening to decrease the waist of the APIs. The talc concentration was kept at 10 % in all the screening formulations to reduce its effect on the mechanical property of the filament. The PEO to PEG 6000 ratio was also kept constant at 1:1. This percentage was reported previously to be sufficient for PEO plasticisation [39]. In the first screening formulation (F1), an equal percentage of each of the three polymers was used. However, the filament produced had a waxy texture and was very brittle. Hence, in the second formulation, TEC was used as a plasticiser and the percentage of E EPO: PEO: PEG was 2:1:1. The filament was printable, but due to high viscosity, it required a high printing temperature of 180 °C, and the tablet was very soft. Therefore, to reduce the viscosity, a lower concentration of PEO was used in the third screening formula, resulting in a filament printable at a lower temperature of 165 °C. Table 3 presents the screening formulation, their printability and processing temperature.

The rheological test for the screening formulations was conducted at 150 °C, and the optimal printing temperature chosen to prevent enalapril degradation was observed at 160 °C. The rheology test shows a direct relationship between the high molecular weight polymer PEO concentration and the shear viscosity. Hence, as the concentration of PEO decreased from F1 to F3, the shear viscosity also decreased. Moreover, all three screening formulations show pseudoplastic behaviour. However, the slope of the complex viscosity-frequency graph also slightly decreases with the decrease in the concentration of PEO, which indicates that PEO has a marginally higher rate of thinning at this temperature than E EPO.

Furthermore, Qahtani et al. mentioned that the viscosity of their formulation had to be lower than 1000 Pa. S to be printed with FFF. However, although the viscosities of both F2 and F3 were below the required threshold at 150 °C, a higher temperature was still necessary to print these formulations. Furthermore, a significant difference has been observed between the temperatures needed for extrusion and printing, as printing demands lower viscosity than the higher viscosity ranges needed for HME. Since thermo-thinning depends on the formulation, this temperature gap can vary accordingly. Fig. 1S in the supplementary data illustrates the relationship between complex viscosity and frequency at 150 °C for the screening formulations.

For the EM-F, a higher drug load and a lower printing temperature than F3 were necessary. Additionally, EM had a plasticising effect on the polymer mixture. Therefore, a higher percentage of talc powder was required to counteract this effect and improve the mechanical properties of the filament. As a result, the total amount of the polymers was reduced to 50 % with a ratio of 6:1:1 of E EPO: PEO: PEG and the talc and EM formed the other 50 %. Using inert fillers like talc, in concentrations between 37.5 % to 50 %, has proven effective in improving the mechanical properties of filaments and printlets made with E EPO [35]. Consequently, talc was used in 35 % of the total weight, which is close to a 1:1 ratio with E EPO, to improve the mechanical integrity of the filament and the printed units. Furthermore, no TEC was used since the enalapril is miscible with E EPO, and there is no need for extra plasticisation. Finally, the concentration of EM was 15 % to achieve the dose of 20 mg per unit. Therefore, as required, the printing temperature for EM-F was set to 150 °C to remain below the degradation temperature of enalapril. Hydrochlorothiazide was formulated with E EPO as well. However, due to its high melting point and the presence of a high concentration of talc, the polymer mobility was limited, which led to improving the mechanical strength of the E EPO without the need for a flexibility modifier. This strategy, which Yang et al. suggested, has proven its effectiveness in improving the printability of E EPO with inert filler and high melting API [35]. Although the printing and extrusion temperatures were high, processing temperature was not a concern for this formulation as with enalapril. Table 4 provides the final formulations for the three antihypertensive formulation systems.

### 3.3. Three-dimensional (3D) printing

Printability was assessed directly using the 3D printer, providing a realistic evaluation of the filament's performance. This approach offers a more practical reflection of true printability compared to indirect methods that rely solely on mechanical property predictions.

The infill densities of EM-U, HCT-U, and PR-U were set to 90 %, 50

**Table 3**
Screening formulations and their printability, extrusion and printing temperature.

| | Eudragit EPO | TEC** | PEO | PEG 6000 | Talc | Printability | Extrusion temp. | Printing temp. |
|---|---|---|---|---|---|---|---|---|
| F 1* | 30 % | 0 % | 30 % | 30 % | 10 % | Brittle | 70 °C | – |
| F 2* | 40.5 % | 4.5 % | 22.5 % | 22.5 % | 10 % | Printable | 80 °C | 180 °C |
| F 3* | 54 % | 6 % | 15 % | 15 % | 10 % | Printable | 70 °C | 165 °C |

*F1, F2 and F3 = formulation 1,2 and 3. ** TEC = triethyl citrate.

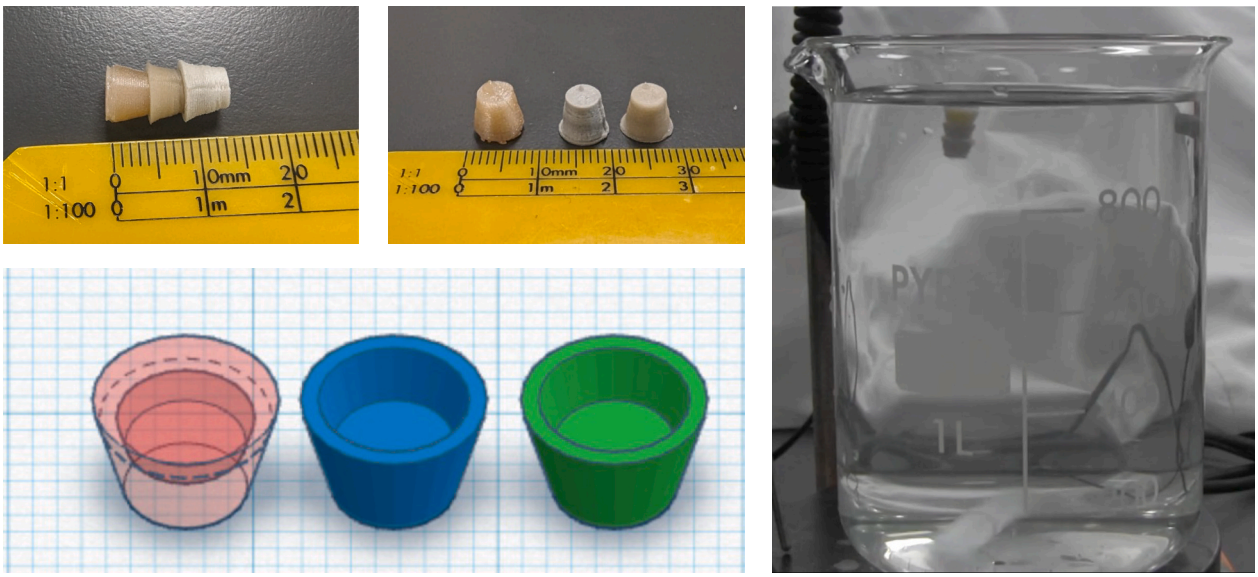

*Figure 1 The design of the FlexiPill units (bottom left), the units after printing(top left) and the floatation in 0.1 N HCl (right side).*

**Fig. 1.** The design of the FlexiPill units (bottom left), the units after printing(top left) and the floatation in 0.1 N HCl (right side).

**Table 4**
The final formulation for the Flexipill units.

| | Eudragit EPO | Eudragit RLPO | TEC | PEO | PEG 4000 | PEG 6000 | Talc | API | Extrusion temp. | Printing temp. |
|---|---|---|---|---|---|---|---|---|---|---|
| EM-F* | 37.5 % | | | 6.25 % | | 6.25 % | 35 % | 15 % | 70 °C | 150 °C |
| HCT-F** | 46.75 % | | 3.25 % | | | | 37.5 % | 12.5 % | 100 °C | 160 °C |
| PR-F*** | | 60 % | | | 10 % | | | 30 % | 70 °C | 160 °C |

* EM-F = enalapril maleate formulation, **HCT-F = hydrochlorothiazide formulation, ***PR-F = propranolol formulation.

%, and 20 %, respectively, to align the doses with the clinical requirements for all three antihypertensive agents. Consequently, as previously proven, the infill or the number of units used can be easily modified to personalise the dose [40]. Fig. 1 shows the design of the Flexipill units, the printed units, and their floatation behaviour in 0.1 N HCl.

### 3.4. Scanning electron microscope

The SEM images of the filaments show that the PR-F filament has a smooth surface with some textural voids and inclusions. However, no propranolol crystals were observed. Moreover, the EM-F filament appeared smoother with no voids but some inclusions. Additionally, the filament cross-section spiral arrangement of the extruded material is more visible due to the presence of talc. Lastly, the HCT-F had much more surface texture and more visible pores. The cross-section again shows the extrudate's spiral arrangement due to the high percentage of talc. Fig. 2S in supplementary data presents the SEM images of the three filaments produced through HME.

Fig. 2 shows the SEM images of the three printed units. PR-U and EM-U show good layer adhesion, with no gaps and uniform layer thickness. However, the HCT-U had less layer uniformity, caused by high viscosity, which led to uniform material extrusion.

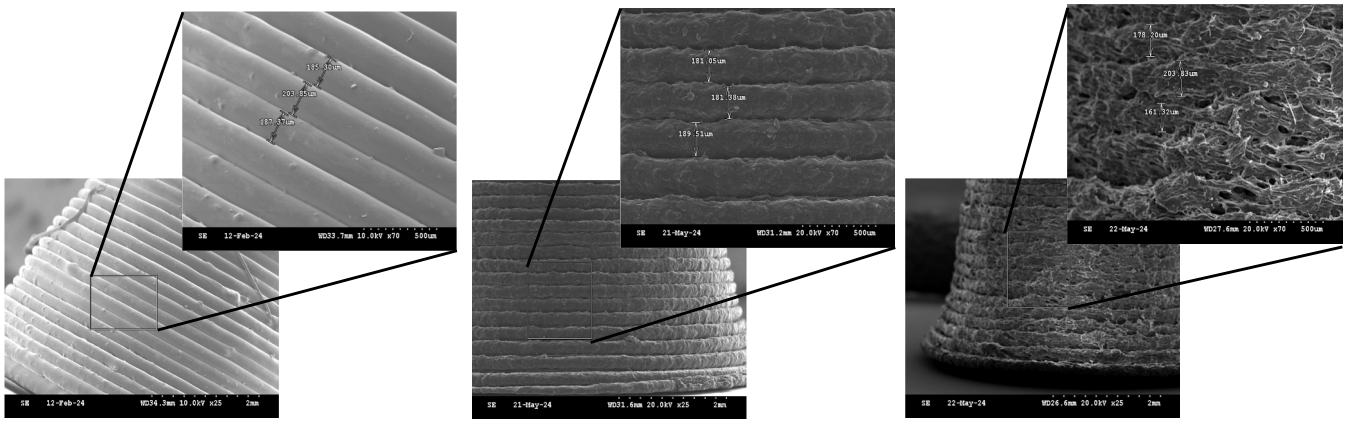

*Figure 2 SEM for the printed units. (A) PR-U, (B) EM-U and (C) HCT-U.*

**Fig. 2.** SEM for the printed units. (A) PR-U, (B) EM-U and (C) HCT-U.

### 3.5. Thermal analysis

Thermogravimetric analysis (TGA) was conducted on all three formulations to evaluate their stability at the processing temperature. TGA of pure EM shows two steps of decomposition the first step corresponds to a 24 % decrease in weight between 156 °C to 221 °C and a peak in the derivatised thermalgravimetric (DTG) curve at 171° C and corresponds to the formation of diketopiperazine by intramolecular cyclisation after the removal of the water and the maleate molecules [41]. The second step is the result of diketopiperazine's complete degradation, which shows a peak degradation rate at 345 °C. Additionally, E EPO also shows a two-step degradation, the first between 236 °C and 331° C with a peak rate at 299 °C. The weight lost in this step is 27.3 %, corresponding to removing the dimethylamino groups from the polymer and forming six-membered cyclic anhydrides [42]. The second step corresponds to the complete degradation of the polymer and peaks at 423 °C. PEO 200 K and PEG 6000 show one-step degradation that peaks around 395° C due to the similarity in the chemical structure. As a result, the DTG of the EM-F shows four degradation steps the first is the formation of diketopiperazine from enalapril that peaks at 218.17 °C, the second is a combination of the complete degradation of enalapril and the removal of the dimethylamino groups from the E EPO that peaks at 291.3 °C, the third step is caused by the degradation of PEG 6000 and PEO 200 K peaking at 383.3 °C and the fourth step is the complete degradation of E EPO peaking at 417.2 °C. TGA confirm the stability of the EM-F at the processing temperature since degradation temperature is higher. Fig. 3S in the supplementary data displays the TGA and DTG results for EM-F and its components.

The PR-F degradation thermogram shows a two-step degradation process. The first starts at 210 °C and peaks at 270° C, with a weight loss of 30 % equivalent to the propranolol concentration in the formulation. The second step peaks at 395 °C and is caused by E RLPO and PEG 4000 degradation. Fig. 4S in the supplementary data illustrates the TGA and DTG profiles for PR-F and its components.

The thermal degradation of HCT-F occurs in two steps. The first, which peaks at 294 °C, corresponds to both the degradation of HCT and the first step of E EPO thermal degradation and the second step, which peaks at 425 °C, is caused by the complete degradation of the polymer. Fig. 5S in the supplementary data displays the TGA and DTG curves for HCT-F and its components.

The TGA results for the three systems indicate that the formulations remain stable at the extrusion and printing temperatures, as the degradation temperatures of all the components are higher than the processing temperature.

In the DSC, propranolol had a sharp endothermic peak at 163.85 °C, corresponding to the melting of propranolol. On the other hand, the PR-U thermograph shows an endothermic peak at 160 °C, indicating that some of the 30 % propranolol in the formulation is still in its crystalline state. Additionally, the other endothermic peak at 57o C results from the melting of PEG 4000. Fig. 3A shows the DSC of the PR-U and PR.

The DSC of enalapril shows two overlapping peaks. The first sharp peak at 149 °C results from the melting of the enalapril crystals and a second broader peak at 160 °C is caused by the degradation of enalapril [43]. However, these peaks do not show in the DSC of the EM-F printlet, indicating that EM has interacted with the polymer, forming an amorphous solid dispersion—the only endothermic peak in the thermograph at 53.4 °C results from the melting of PEG 6000. Fig. 3B displays the DSC of the EM-U and pure EM.

Finally, the DSC of HCT-F could not be used to show the presence of hydrochlorothiazide melting peak since degradation of the methacrylate polymer at 250 °C interfered with the melting signal of hydrochlorothiazide at 267 °C. Fig. 3C shows the DSC of the HCT-U and pure HCT.

### 3.6. Fourier transform infrared

Thereafter, the FTIR spectrum was investigated to find any interaction between the APIs and the polymers. If the formulation spectrum shows a shift or disappearance of the band from the API spectrum, this is

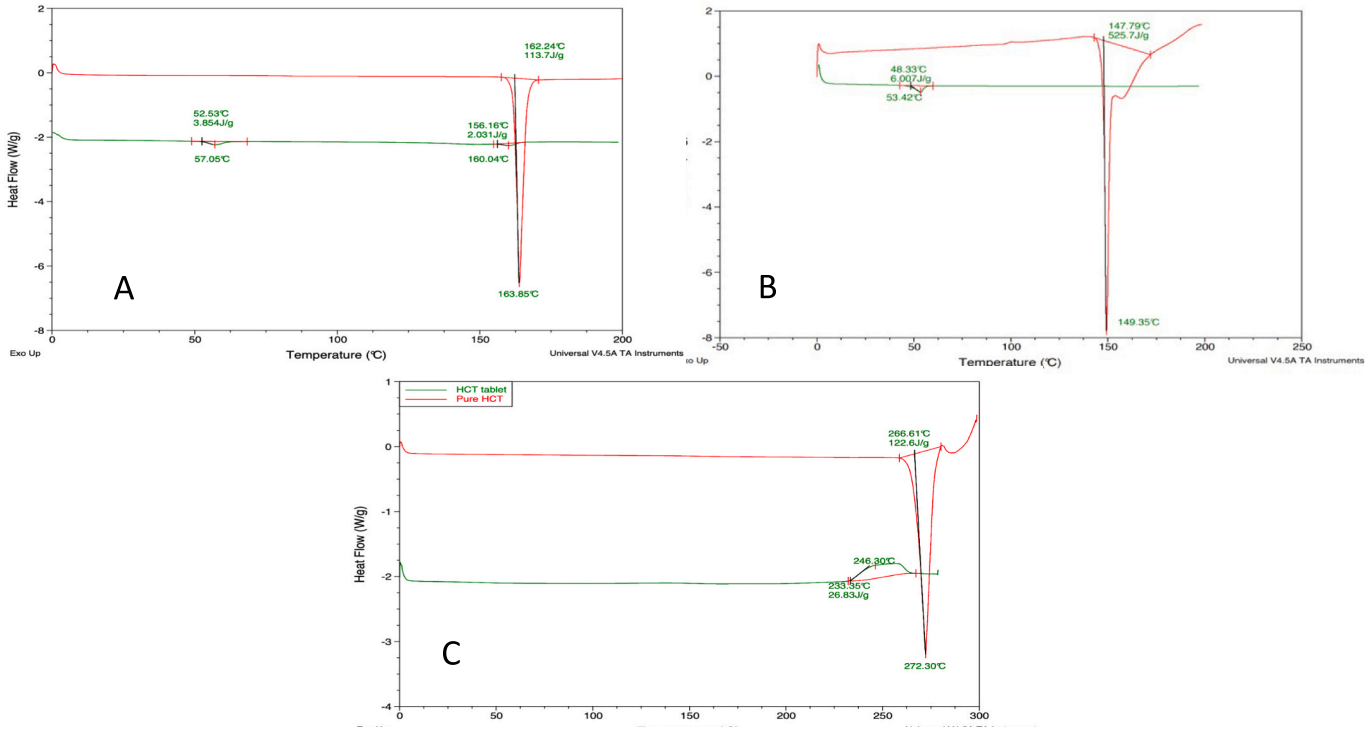


*Figure 3 Differential scanning calorimetry for the printed units (green) and the pure APIs (red). (A) PR-F and propranolol, (B) EM-F and Enalapril and (C) HCT-F and Hydrochlorothiazide.*

**Fig. 3.** Differential scanning calorimetry for the printed units (green) and the pure APIs (red). (A) PR-F and propranolol, (B) EM-F and Enalapril and (C) HCT-F and Hydrochlorothiazide. (For interpretation of the references to colour in this figure legend, the reader is referred to the web version of this article.)

a sign of supramolecular interactions. The propranolol FTIR spectrum band at 1265.3 $cm^{-1}$, which corresponds to the stretch of the C-O in the ether group, shows no shift in the formulation spectrum. However, the band assigned to the aromatic C–C stretching at 1577.7 $cm^{-1}$ shifted to 1581.6 $cm^{-1}$ in the formulation spectrum. Additionally, C–H stretching, shown as a band at 2924.1 $cm^{-1,}$ shifts to 2916.3 $cm^{-1}$ in the PR-F spectrum [44]. Moreover, the secondary amine group presence as a band at 2972.3 $cm^{-1}$ in the propranolol spectrum also shifts to 2978.1 $cm^{-1}$. Lastly, the band at 3277 $cm^{-1}$ assigned to the hydroxyl group is broadened in the formulation spectrum due to the formation of the H-bond [45]—all these alterations in the propranolol spectrum, indicating a supramolecular interaction between it and E RLPO. Fig. 4A compares the FTIR spectra of the PR printed units with that of pure PR.

In the EM spectrum, the peak at 3,211.48 $cm^{-1,}$ corresponding to stretching vibrations of N–H, disappears in the formulation spectrum—additionally, the band at 2,980.02 $cm^{-1}$ assigned to asymmetric $CH_3$ stretching vibration shifts to 2,970.38 $cm^{-1}$. Furthermore, the band at 1,749.44 $cm^{-1}$ caused by the carbonyl stretching of ester disappeared, and the carboxylic acid peak at 1,724.36 $cm^{-1}$ shifted to 1,726.29 $cm^{-1}$ in the formulation spectrum. The carbonyl stretching of the tertiary amide at 1,645.28 also shifts to 1,668.43 in the formulation [46]. The FTIR spectrum confirms DSC's finding and proves EM's complete miscibility in the methyl acrylate polymer. Fig. 4B compares the FTIR spectra of the EM printed units with that of pure EM.

Finally, in the spectrum of pure HCT, the asymmetric and symmetric vibrations of the sulphonyl groups are visible at 1,315.45 $cm^{-1}$ and 1,147.65 $cm^{-1}$, respectively. Both bands decrease in intensity and shift to 1,319.31 $cm^{-1}$ and 1,134.14 $cm^{-1}$, respectively [29]. The NH stretching of the sulphonamide and amine groups, which appears at 3,356.14 $cm^{-1}$, 3,265.49 $cm^{-1}$ and 3,169.04 $cm^{-1}$, does not shift, but the band intensity decreases in the IR spectrum of the formulation. The CH2 stretching at 2,987.74 $cm^{-1}$ and 2,900.94 $cm^{-1}$ does not change in the formulation spectrum [47]. Additionally, the C=C stretching at 1,595.13 $cm^{-1}$ and 1,516.05 $cm^{-1}$ decrease in intensity and shift to 1,589.34 $cm^{-1}$ and 1,512.19 $cm^{-1}$, respectively, indicating potential molecular interactions. As a result, the FRIR data reveals an interaction between the HCT and the E EPO, as reported previously [48]. Fig. 4C compares the FTIR spectra of the HCT printed units with that of pure HCT.

### 3.7. Powder X-ray diffraction

When analysing the Powder x-ray diffraction pattern HCT-U, the presence of a diffraction peak at 21.33° 2θ in the pure HCT powder and its absence in the HCT printed unit (HCT-U) and the physical mixture confirms the transformation of HCT crystal into an amorphous solid dispersion upon mixing before processing. Meanwhile, the other peaks corresponding to the diffraction pattern of talc are still present. On the other hand, the diffraction pattern of PR-U, pure PR, and the preprint powder mixture all show the presence of propranolol crystal, confirming that the DSC results of partial crystallinity are retained after processing. Finally, the diffraction pattern of the Enalapril printed unit also shows only the diffraction peaks of talc, confirming the formation of amorphous solid dispersion. Fig. 5 compares the X-ray diffraction patterns of the printed units, the pure APIs and the formulation physical mixtures.

### 3.8. Rheological study

The FFF process depends on heating the filament to a temperature in which the thermoelastic polymer turns from an elastic to a viscous state

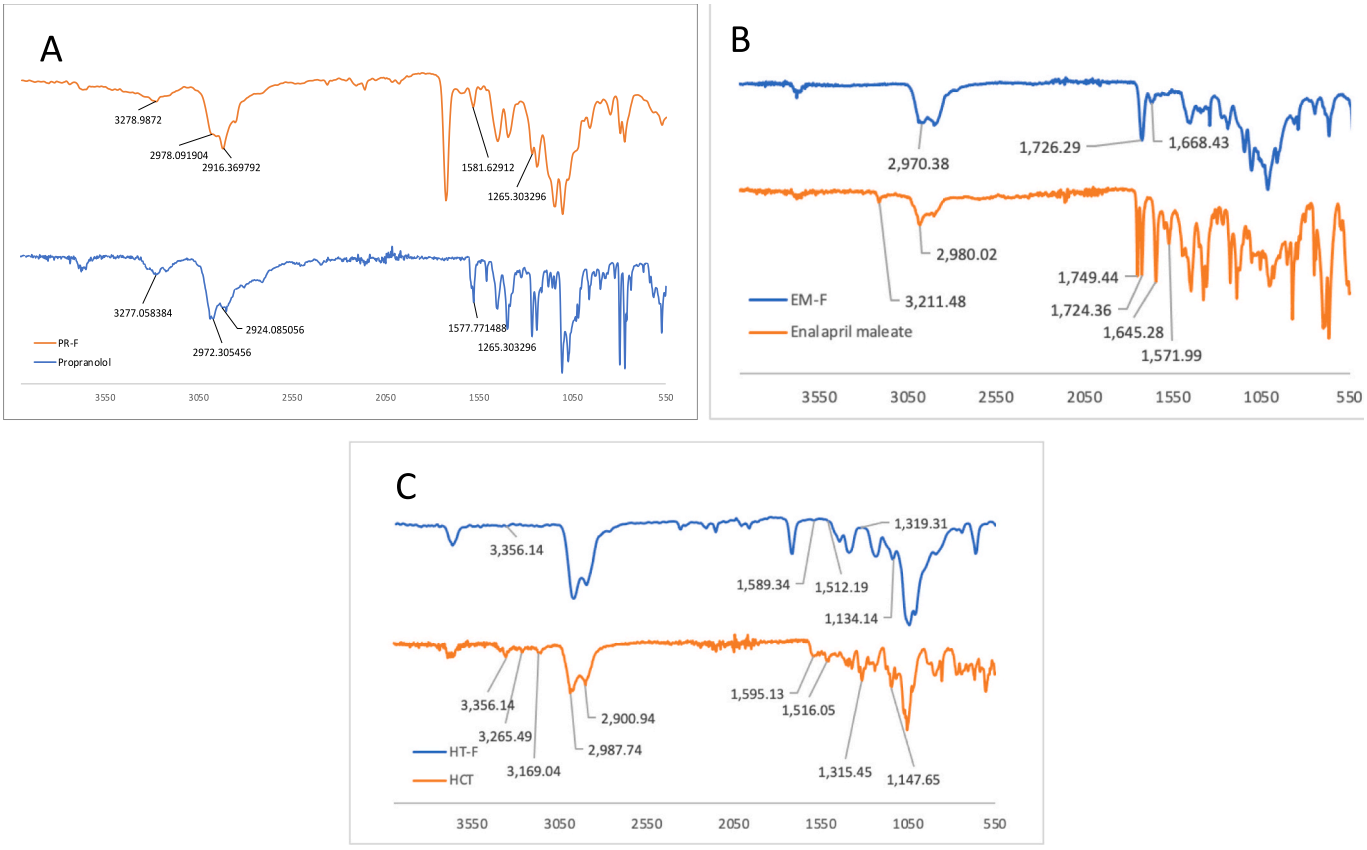


*Figure 4 FTIR spectrum for the printed units and the pure APIs. (A) PR-F and propranolol, (B) EM-F and Enalapril and (C) HCT-F and Hydrochlorothiazide.*

**Fig. 4.** FTIR spectrum for the printed units and the pure APIs. (A) PR-F and propranolol, (B) EM-F and Enalapril and (C) HCT-F and Hydrochlorothiazide.

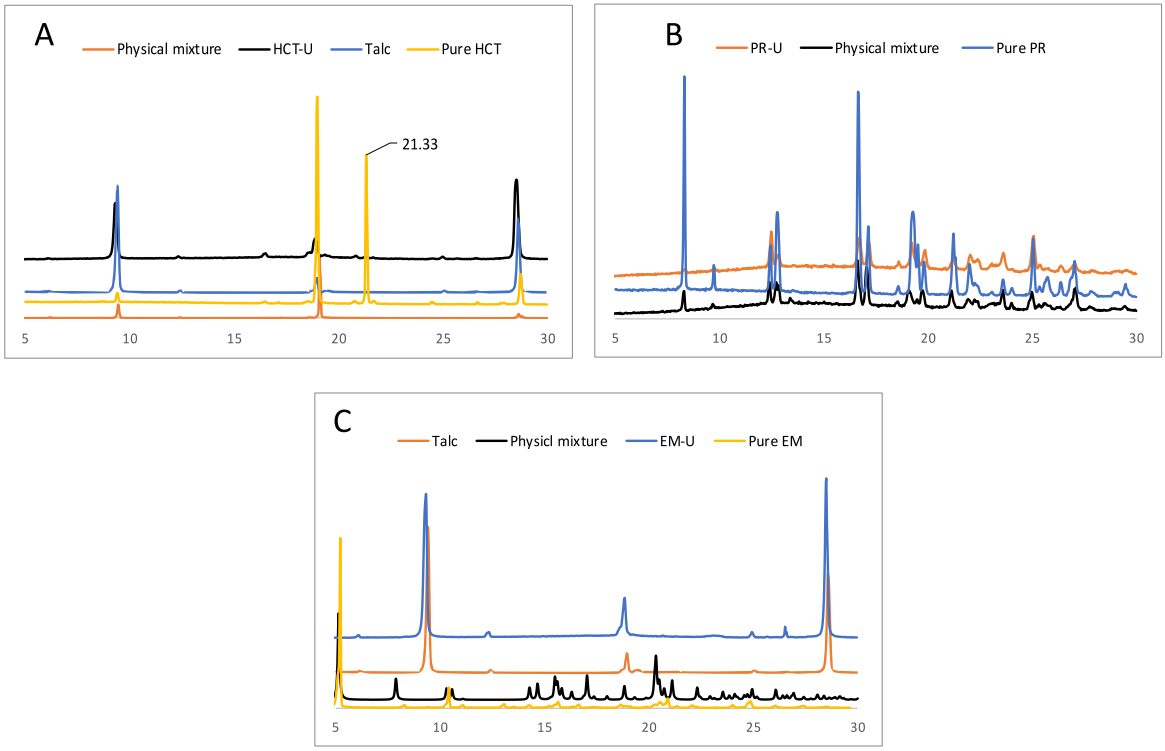


*Figure 5 X-ray diffraction comparing the physical mixture and pure APIs to the printed units. (A) HCT-U, (B) PR-U and (C) EM-U*

**Fig. 5.** X-ray diffraction comparing the physical mixture and pure APIs to the printed units. (A) HCT-U, (B) PR-U and (C) EM-U.

to flow through the narrow nozzle of the printer under high shear. As a result, studying the viscoelastic behaviours of the formulation is an essential step to understanding the printing process. However, learning the rotational viscosity under steady shear is limited to low frequency due to flow disruption and sample rupture. However, according to the Cox-Merz rule, there is an empirical correlation between the viscosity under steady shear and the complex viscosity under oscillatory shear [49].

Therefore, a frequency sweep with fixed strain was used to test the formulation's viscoelastic behaviour. The strain was fixed to 1 % to keep the test within the linear viscoelastic region (LVR). The temperature was set to the printing temperature for each formulation. Lastly, to determine the apparent shear rate at the printing nozzle, the volume flow rate was calculated from the pre-set printing speed and the nozzle radius, which was 11 $mm^3/s$. Thereafter, the apparent shear rate at the printing nozzle was calculated using the equation:

$$g_{app} = 4Q/\pi R^3$$

where $\gamma_{app}$ is the apparent shear, Q is the volumetric flow rate, and R is the radius of the nozzle.

The apparent shear rate was 533 $Sec^{-1}$. As a result, high frequency was used for the comparison. The test reveals that the mean complex component of the shear *viscosity (SV)* for the PR-F, EM-F and HCT-F were 98.15, 122.6 and 341.5 Pa. S at printing temperature and frequency 100 Hz, respectively. In conclusion, using a high percentage of the inert filler talc in the HCT-F to improve the mechanical properties of E EPO led to higher viscosity. This contrasts with the approach used in the EM-F, where inert filler and polymer blends were used, hence the high printing temperature for HCT-F. Moreover, these results align with the value set by Qahtani et al.. for printing PLA, between 1000 Pa. S to 100 Pa. S. [50]. Additionally, the shear index, the parameter used to describe the flow of non-Newtonian fluids in response to applied shear forces for HCT-F and EM-F, was less than 1. This indicates that both formulations displayed shear thinning, as evidenced by increased viscosity with decreased frequency. However, PR-F shows a decrease in viscosity as the frequency decreases to 25 Hz because, at high frequency, the behaviour of E RLPO is dominated by the elastic response due to entanglement of the polymer chains, leading to higher complex viscosity. As the frequency decreases, these entanglements can relax, and an increase in the viscosity with decreasing frequency can be observed. This behaviour can be observed in the relatively high shear index for PR-F. Finally, in the PR-F formulation, the loss modulus was higher than the storage modulus at low frequencies. Still, it became equal to or lower than the storage modulus at high frequency. This confirms the entanglement of the polymer chain at high frequency, which can store the energy of the deformation. In contrast, the polymer chains are more relaxed at low frequencies, and energy dissipates as heat, acting like a liquid. On the other hand, the EM-F and HCT-F storage modulus is lower than the loss modulus at any frequency. Fig. 6 presents the complex viscosity, loss modulus, and storage modulus as frequency functions, along with the shear index.

### 3.9. Chromatography

One challenge in adapting polypills is finding reliable analytical methods for qualitative and quantitative analysis. When developing the HPLC method, phenyl-hexyl column was used instead of a C18 column because no separation was observed between propranolol and enalapril on the C18. However, due to the phenyl-hexyl column's affinity for π–π interactions, enalapril exhibited a longer retention time, resulting in improved separation from propranolol. The method developed achieved adequate separation between maleate, HCT, propranolol, and enalapril, with retention times of 1.48, 2.49, 9.42, and 10.42 min, respectively, and a total run time of 15 min. However, since enalapril has a lambda max at a low wavelength, the DAD was set to measure two signals, 210 nm and 280 nm. Nevertheless, the baseline at these wavelengths was not ideal due to solvent interference. Therefore, for HCT and propranolol, a 280 nm signal was employed for more accurate detection.

Additionally, LC-MS was utilised for the final data point in the

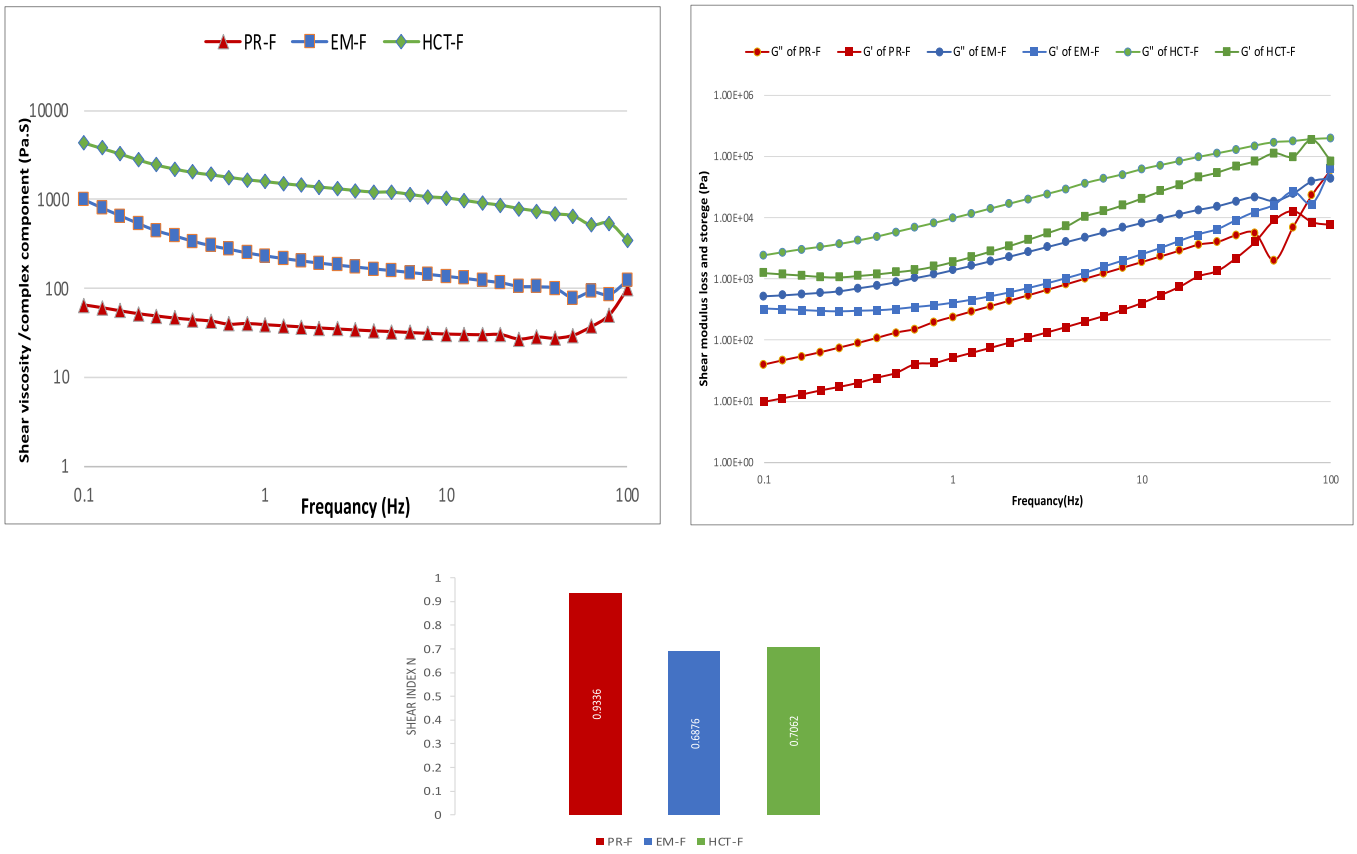


*Figure 6 Complex viscosity versus angular frequency of the three formulations at their perspective printing temperature(left), loss and storage modulus versus frequency (right) and Shear index for the three formulations (bottom).*

**Fig. 6.** Complex viscosity versus angular frequency of the three formulations at their perspective printing temperature(left), loss and storage modulus versus frequency (right) and Shear index for the three formulations (bottom).

dissolution test and drug content analysis to assess any degradation resulting from the dissolution medium and processing (extrusion and printing), respectively. In both instances, the peaks exclusively corresponded to the API mass, with no detectable degradants. Fig. 6S in the supplementary data shows the HPLC method chromatograms with the MS peaks.

### 3.10. Drug content and dissolution test

Furthermore, the analysis of drug content shows that the theoretical and experimental drug concentrations are consistent, as seen in Table 2, indicating that there was no weight loss or degradation during the processing of any formulation. In the dissolution apparatus, the paddle rotation was set to 100 RPM to evaluate the floating of the tablets under vigorous conditions. However, the tablet floated immediately upon being placed in the dissolution medium. After 30 min, the HCT-U and EM-U units disconnected from the floating PR-U and began to sink. Nevertheless, the dissolution test for the HCT-U and EM-U continued in the acidic dissolution medium because the units started to erode, making them impossible to remove after 2–3 h to simulate gastric emptying. The PR unit remained afloat for over 9 h, after which the dissolution medium penetrated the unit due to the separation of the printed layers.

Several release models were examined to identify the optimal fit for drug release from the three units. The zero-order model was considered because it describes concentration-independent release, which is typical in sustained-release formulations. The first-order model is common for immediate-release formulations, where the release is concentration-dependent. Higuchi's model describes diffusion-controlled release observed in polymeric matrices, while the Hopfenberg model explains release through erosion from a polymeric matrix. Finally, the Korsmeyer-Peppas model was utilised as a mathematical tool to describe the release with a release exponent (n), providing insight into whether drug release follows Fickian diffusion, anomalous transport, or Case-II transport [51]. Two approaches were employed to determine the best model among these: the correlation coefficient ($R^2$) and the Akaike Information Criterion (AIC). While the correlation coefficient can lead to overfitting, AIC penalises overfitting; it depends on the number of samples and is only useful for comparing models without providing insight into the model's quality. Therefore, both approaches were utilised [52].

The drug release was conducted for 24 h because propranolol release was expected to have prolonged release. Propranolol release from the E RLPO matrix follows concentration-dependent release (first-order release kinetics). The release model fitting was conducted for the initial 6 h, after which drug release reached a steady state. Compared to the other models, the release fits the first-order kinetics, $R^2 = 0.98$ and AIC = 27.46. Table 5 lists the fitting of the kinetic models to the release profile of the three units. Additionally, the Korsmeyer-Peppas release exponent (n) is 0.47, falling within the range of 0.45 to 0.89, which indicates that the release follows a non-Fickian anomalous transport model [53]. As a result, propranolol release can be described as a non-Fickian diffusion that does not depend on the concentration gradient alone but on the drug's concentration. The dissolution medium penetrates through the polymer matrix, causing it to swell and relax. While the outer part of the matrix releases the drug faster, the centre of the matrix releases the drug slower due to the longer path the drug needs to

**Table 5**
Fitting a release model for the release of the three units of the Flexipill.

| | ZOM prediction correlation ($R^2$) | AIC for ZOM | FOM prediction correlation ($R^2$) | AIC FOR FOM | HIG-M PREDICTION CORRELATION ($R^2$) | AIC for HIG-M | HOP-M PREDICTION correlation ($R^2$) | AIC FOR HOP-M | K-P M PREDICTION correlation ($R^2$) | AIC FOR K-P M | K-P M release exponent (n) |
|---|---|---|---|---|---|---|---|---|---|---|---|
| PR-U release | 0.85 | 42.78 | **0.98** | **27.46** | 0.93 | 49.07 | 0.92 | 46.32 | 0.93 | 37.80 | 0.47 |
| EM-U release | 0.78 | 39.80 | **0.96** | **25.43** | 0.86 | 54.66 | 0.91 | 51.70 | 0.90 | 40.45 | 0.29 |
| HCT-U release ($R^2$) | 0.79 | 38.77 | **0.98** | **23.66** | 0.88 | 34.95 | 0.98 | 27.31 | 0.90 | 34.43 | 0.37 |

AIC = AKAIKE Information Criterion, ZOM = ZERO-ORDER MODEL, FOM = FIRST-ORDER MODEL, HIG-M= HIGUCHI'S MODEL, HOP-M= HOPFENBERG'S MODEL, K-P M = Korsmeyer-Peppas model.

take to be eluted through the nonhomogeneous matrix [54]. Therefore, as time progresses, the remaining drug concentration decreases, and the release rate decreases. The European Medicines Agency (EMA) uses the biopharmaceutics classification system (BCS) to guide immediate or sustained release oral dosage forms. The BCS classify drug molecules into four classes according to their solubility and permeability. Propranolol is classified as a class I BCS [55]. According to EMA guidelines, the specification for in vitro dissolution of an oral prolonged-release product should include at least three key time points: an early time point to rule out dose dumping and/or characterise the loading or initial dose (typically 20–30 % dissolved), at least one intermediate point to verify the dissolution profile's shape (around 50 % dissolved), and a final point to confirm that the majority of the active substance has been released (Q = 80 %) [56]. The objective for the PR-U was to have a prolonged release, and a complete drug release occurs while the unit is still floating. In the first three points up to the 30-minute time point, there was no drug dumping the average release was 19 %, 52 % release was achieved at the 60-minute time point, and drug release was prolonged to 9 h, and 96.6 % was released before flotation ended. Fig. 7A presents the accumulative release of propranolol from PR-U in the dissolution test.

On the other hand, enalapril is classified as a class III BCS with high solubility but low permeability [57]. Its release can be divided into two phases. Phase one, in which drug release is governed mainly by erosion of the polymer matrix, shows high drug release in the first 60 min and releases more than 60 % of the drug. In phase two, drug release is mainly through slow diffusion from the eroded unit segments. The maximum drug release that an EM-U reaches in 24 h is 80 %. The release model fitting for enalapril over the 24 h showed the best fit with first-order kinetics $R^2$ = 0.96 and AIC = 25.43. However, the release rate exponent (n) of the Korsmeyer-Peppas release model is 0.29, which is less than 0.45, indicating a Fickian diffusion. The EM-U formulation did not achieve immediate release, likely due to the presence of high molecular weight PEO. This polymer slowed the second drug release phase, governed by diffusion, as enalapril must travel through extended paths within the long polymer chains. Fig. 7B presents the accumulative release of enalapril from EM-U in the dissolution test.

Hydrochlorothiazide is classified as a class II BCS with low solubility and good permeability [29]. The HCT release from its unit was relatively fast, reaching over 80 % release after 60 min and 100 % release after 6 h. The 9-hour time point showed a high standard deviation that raised the release value slightly above 100 %. In conventional tablet, only 64 % is release in the first 60 min [58]. The European Medicines Agency considers 75 % drug release of the labelled drug in the first 45 min are the defining criteria for an immediate release formulation, according to this definition, HCT-F could be considered as such [59]. Drug release is mainly governed by the quick erosion of the cationic methacrylate copolymer in the acidic medium. There was no diffusion phase as witnessed in the EM-U since this formulation contains no PEO 200 K, which slowed the release of the API in the enalapril formulation. The erosion of the matrix is homogenous, meaning that the erosion rate depends on the amount of polymer remaining. As a result, the drug release from HCT-U during the initial 4 h before reaching a steady state follows the first-order kinetic model $R^2$ = 0.98 and AIC = 23.66. Fig. 7C presents the accumulative release of HCT from HCT-U in the dissolution test with the kinetic model fitting.

## 4. Conclusion and future perspective

The high prevalence of hypertension worldwide causes a significant burden on the healthcare system and, if not controlled, can lead to other cardiovascular complications. Hypertension is a multifactorial disease. Hence, treatment with multiple antihypertensive agents is required at the same time. As a result, the fixed-dose combination was suggested to improve patient compliance with such a high number of medications. However, due to many limitations of FDC, a Flexible dose combination that can be personalised according to patient needs has become a need for the healthcare system, especially for chronic diseases that require polypharmacy, like hypertension. Such a formulation can improve patient adherence to treatment and, as a result, ameliorate the clinical outcome of the treatment. Recent advancements in additive manufacturing can pave the way for more intricate designs and shorten the path to personalised medication.

In this work, Flexipill, a flexible polypill for hypertension that can be assembled at the point of care according to patient needs, was designed and printed using Fused filament fabrication. The Flexipill contained three antihypertension medications: propranolol, which was formulated as a floating unit that released the drug by diffusion with prolonged release; the thermolabile drug enalapril did not achieve immediate release, however this was not the primary objective of this research, but the objective was to lower the printing temperature to avoid thermal degradation; and hydrochlorothiazide, which was printed as an immediate-release unit. Accordingly, the development of immediate release formulation for Enalapril using the technique applied in this work need to be considered in the future.

This work demonstrates the capability of this new dosage form to administer more than one therapeutic agent to patients with chronic disease and personalise the combination, the dose, and the release according to each patient at the point of care. In the future, this can bridge the gap between the need for treatment personalisation and regulatory concerns over having a printer at the point of care.

## CRediT authorship contribution statement

**Yasir Karkar:** Writing – original draft, Visualization, Validation, Methodology, Investigation, Formal analysis, Data curation, Conceptualization. **Tanzeela Anis:** Investigation, Data curation. **Amal Ali Elkordy:** Writing – review & editing, Supervision, Validation. **Ahmed Faheem:** Writing – review & editing, Supervision, Project administration.

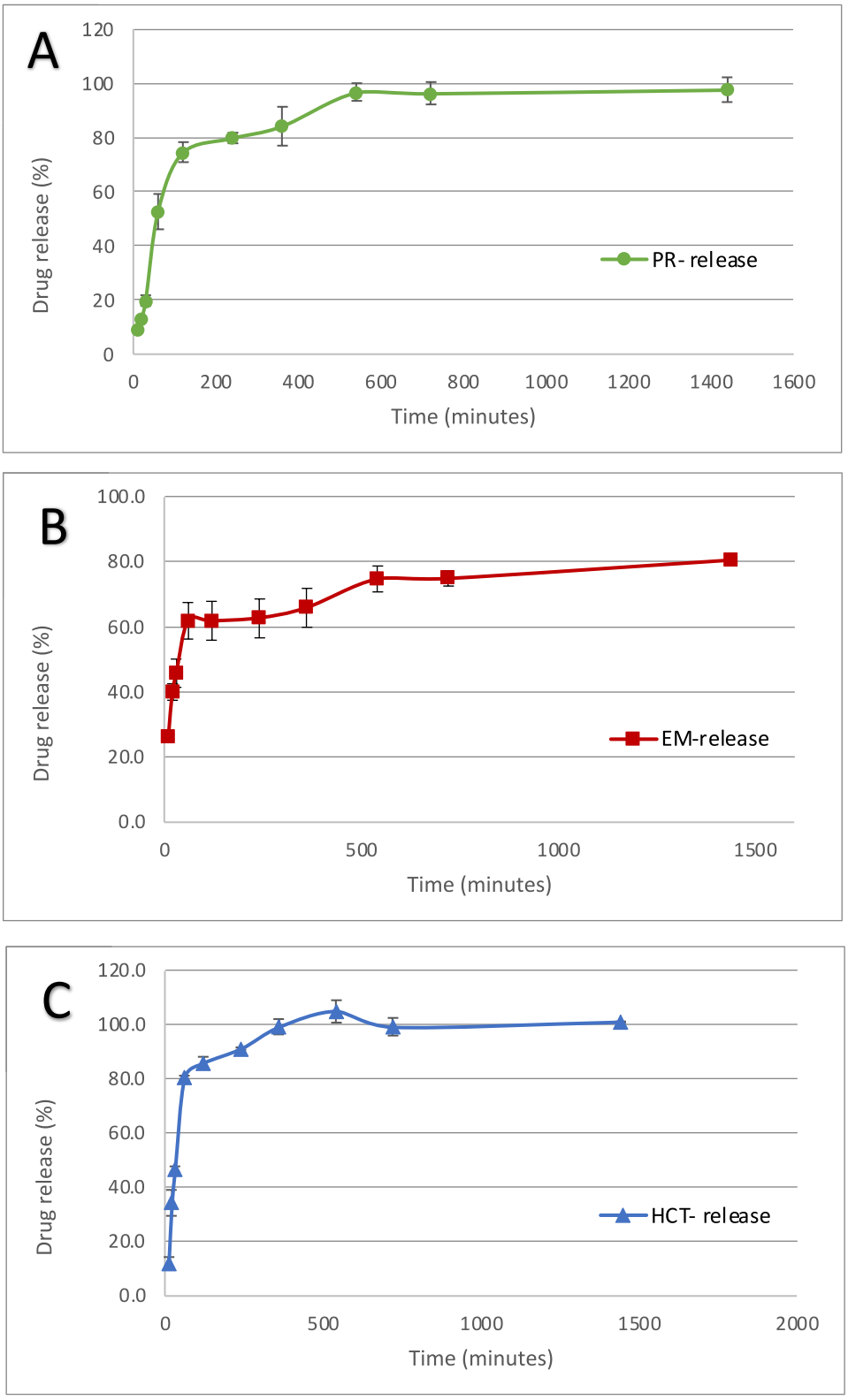


*Figure 7 Drug release from the printed units in the dissolution test; (A) PR-U, (B) EM-U and (C) HCT-U.*

**Fig. 7.** Drug release from the printed units in the dissolution test; (A) PR-U, (B) EM-U and (C) HCT.

## Declaration of competing interest

The authors declare that they have no known competing financial interests or personal relationships that could have appeared to influence the work reported in this paper.

## Appendix A. Supplementary data

Supplementary data to this article can be found online at https://doi.org/10.1016/j.ejpb.2025.114736.

## Data availability

Data will be made available on request.

## References


[1] P.M. Kearney, et al., Global burden of hypertension: analysis of worldwide data, Lancet 365 (9455) (2005) 217–223.
[2] G.S. Stergiou, Combination pharmacotherapy in hypertension, Int. Urol. Nephrol. 38 (2006) 673–682.
[3] G. Stergiou, et al., Aggressive blood pressure control in general practice (ABC-GP) study: can the new targets be reached? J. Hum. Hypertens. 17 (11) (2003) 767–773.
[4] J. Amar, et al., Hypertension in high-risk patients: beware of the underuse of effective combination therapy (results of the PRATIK study), J. Hypertens. 20 (4) (2002) 779–784.
[5] B.N. Mukete, K.C. Ferdinand, Polypharmacy in older adults with hypertension: a comprehensive review, J. Clin. Hypertension 18 (1) (2016) 10–18.
[6] G. Mancia, G. Grassi, Systolic and diastolic blood pressure control in antihypertensive drug trials, J. Hypertens. 20 (8) (2002) 1461–1464.
[7] B. Williams, et al., 2018 ESC/ESH Guidelines for the management of arterial hypertension: The Task Force for the management of arterial hypertension of the European Society of Cardiology (ESC) and the European Society of Hypertension (ESH), Eur. Heart J. 39 (33) (2018) 3021–3104.
[8] T. Unger, et al., 2020 International Society of Hypertension global hypertension practice guidelines, Hypertension 75 (6) (2020) 1334–1357.
[9] A.H. Gradman, et al., Combination therapy in hypertension, J. Am. Soc. Hypertens. 4 (2) (2010) 90–98.
[10] D. Smith, et al., 3D printed capsules for quantitative regional absorption studies in the GI tract, Int. J. Pharm. 550 (1–2) (2018) 418–428.
[11] D.K. Smith, R.P. Lennon, P.B. Carlsgaard, Managing hypertension using combination therapy, Am. Fam. Physician 101 (6) (2020) 341–349.
[12] J. Yeaw, et al., Comparing adherence and persistence across 6 chronic medication classes, J. Manag. Care Pharm. 15 (9) (2009) 728–740.
[13] A.N. de Cates, et al., Fixed-dose combination therapy for the prevention of cardiovascular disease, Cochrane Database Syst. Rev. 4 (2014).
[14] N.J. Wald, et al., Cost–benefit analysis of the polypill in the primary prevention of myocardial infarction and stroke, Eur. J. Epidemiol. 31 (2016) 415–426.
[15] P.C. Group, An international randomised placebo-controlled trial of a four-component combination pill ("polypill") in people with raised cardiovascular risk, PLoS One 6 (5) (2011) e19857.
[16] A. Roy, N. Naik, K. Srinath Reddy, Strengths and limitations of using the polypill in cardiovascular prevention, Curr. Cardiol. Rep. 19 (2017) 1–8.
[17] M. Sadia, et al., From 'fixed dose combinations' to 'a dynamic dose combiner': 3D printed bi-layer antihypertensive tablets, Eur. J. Pharm. Sci. 123 (2018) 484–494.
[18] B.C. Pereira, et al., 'Temporary Plasticiser': A novel solution to fabricate 3D printed patient-centred cardiovascular 'Polypill'architectures, Eur. J. Pharm. Biopharm. 135 (2019) 94–103.
[19] P. Robles-Martinez, et al., 3D printing of a multi-layered polypill containing six drugs using a novel stereolithographic method, Pharmaceutics 11 (6) (2019) 274.
[20] S.A. Khaled, et al., 3D printing of five-in-one dose combination polypill with defined immediate and sustained release profiles, J. Control. Release 217 (2015) 308–314.
[21] S. Cailleaux, et al., Fused Deposition Modeling (FDM), the new asset for the production of tailored medicines, J. Control. Release (2020).
[22] P.K. Bg, et al., 3D printing in personalized medicines: A focus on applications of the technology, Mater. Today Commun. (2023) 105875.
[23] K. Englezos, et al., 3D printing for personalised medicines: implications for policy and practice, Int. J. Pharm. 635 (2023) 122785.
[24] R.M. Cooper-DeHoff, et al., Antihypertensive drug class interactions and risk for incident diabetes: a nested case–control study, J. Am. Heart Assoc. 2 (3) (2013) e000125.
[25] D. Chen, et al., Preparation and in vitro evaluation of FDM 3D-printed ellipsoid-shaped gastric floating tablets with low infill percentages, AAPS PharmSciTech 21 (1) (2020) 1–13.
[26] K. Ilyés, et al., 3D floating tablets: Appropriate 3D design from the perspective of different in vitro dissolution testing methodologies, Int. J. Pharm. 567 (2019) 118433.
[27] S. Lamichhane, et al., Customized novel design of 3D printed pregabalin tablets for intra-gastric floating and controlled release using fused deposition modeling, Pharmaceutics 11 (11) (2019) 564.
[28] L. Hoffmann, J. Breitkreutz, J. Quodbach, Fused deposition modeling (FDM) 3D printing of the thermo-sensitive peptidomimetic drug enalapril maleate, Pharmaceutics 14 (11) (2022) 2411.
[29] M. Ruponen, H. Rusanen, R. Laitinen, Dissolution and permeability properties of co-amorphous formulations of hydrochlorothiazide, J. Pharm. Sci. 109 (7) (2020) 2252–2261.
[30] M.R. Symonds, A. Moussalli, A brief guide to model selection, multimodel inference and model averaging in behavioural ecology using Akaike's information criterion, Behav. Ecol. Sociobiol. 65 (2011) 13–21.
[31] L.A. Melnyk, M.O. Oyewumi, Integration of 3D printing technology in pharmaceutical compounding: Progress, prospects, and challenges, Annals of 3D Printed Medicine 4 (2021) 100035.
[32] N. Beer, et al., Magistral compounding with 3D printing: a promising way to achieve personalized medicine, Ther. Innov. Regul. Sci. 57 (1) (2023) 26–36.
[33] C.N. Patra, et al., Pharmaceutical significance of Eudragit: A review, Future J. Pharm. Sci. 3 (1) (2017) 33–45.
[34] M. Sadia, et al., Adaptation of pharmaceutical excipients to FDM 3D printing for the fabrication of patient-tailored immediate release tablets, Int. J. Pharm. 513 (1–2) (2016) 659–668.
[35] Y. Yang, et al., Strategies and mechanisms to improve the printability of pharmaceutical polymers Eudragit® EPO and Soluplus®, Int. J. Pharm. 599 (2021) 120410.
[36] N. Gottschalk, et al., Brittle polymers in Fused Deposition Modeling: An improved feeding approach to enable the printing of highly drug loaded filament, Int. J. Pharm. 597 (2021) 120216.
[37] Y.M. Than, V. Titapiwatanakun, Tailoring immediate release FDM 3D printed tablets using a quality by design (QbD) approach, Int. J. Pharm. 599 (2021) 120402.
[38] M. Alhijjaj, P. Belton, S. Qi, An investigation into the use of polymer blends to improve the printability of and regulate drug release from pharmaceutical solid dispersions prepared via fused deposition modeling (FDM) 3D printing, Eur. J. Pharm. Biopharm. 108 (2016) 111–125.
[39] A. Isreb, et al., 3D printed oral theophylline doses with innovative 'radiator-like'design: Impact of polyethylene oxide (PEO) molecular weight, Int. J. Pharm. 564 (2019) 98–105.
[40] Y. Karkar, A.A. Elkordy, A.M. Faheem, 3D printed flexible design for personalised drug release, Br. J. Pharm. 8 (2) (2023).
[41] S.M.M. de Souza, et al., Evaluation of thermal stability of enalapril maleate tablets using thermogravimetry and differential scanning calorimetry, J. Therm. Anal. Calorim. 123 (2016) 1943–1949.
[42] N.N. Porfiryeva, et al., Acrylated Eudragit® E PO as a novel polymeric excipient with enhanced mucoadhesive properties for application in nasal drug delivery, Int. J. Pharm. 562 (2019) 241–248.
[43] L. Hoffmann, J. Breitkreutz, J. Quodbach, Hot-melt extrusion of the thermo-sensitive peptidomimetic drug enalapril maleate, Pharmaceutics 14 (10) (2022) 2091.
[44] Z.H. Farooqi, H.Y. Aboul-Enein, IR and UV/visible spectra of propranolol and some fluorinated derivatives: Comparison of experimental and calculated values, Biospectroscopy 2 (2) (1996) 131–141.
[45] C. Patra, et al., Design and evaluation of sustained release bilayer tablets of propranolol hydrochloride, Acta Pharm. 57 (4) (2007) 479–489.
[46] S.-Y. Lin, et al., Intramolecular cyclization of diketopiperazine formation in solid-state enalapril maleate studied by thermal FT-IR microscopic system, Eur. J. Pharm. Biopharm. 54 (2) (2002) 249–254.
[47] A.A. Sultan, et al., Self dispersing mixed micelles forming systems for enhanced dissolution and intestinal permeability of hydrochlorothiazide, Colloids Surf. B Biointerfaces 149 (2017) 206–216.
[48] Z. Senta-Loys, J. Kelleher, D. Jones, Hot-Melt Co-Extrusion Technology as a Platform for Manufacturing of Fixed-Dose Combinations with Differing Release Behaviour for the Treatment of Hypertension.
[49] J. Aho, et al., Roadmap to 3D-printed oral pharmaceutical dosage forms: feedstock filament properties and characterization for fused deposition modeling, J. Pharm. Sci. 108 (1) (2019) 26–35.
[50] M. Qahtani, et al., Experimental design of sustainable 3D-printed poly (lactic acid)/biobased poly (butylene succinate) blends via fused deposition modeling, ACS Sustain. Chem. Eng. 7 (17) (2019) 14460–14470.
[51] A. Talevi, M.E. Ruiz, Drug Release, in: The ADME Encyclopedia: A Comprehensive Guide on Biopharmacy and Pharmacokinetics, Springer International Publishing, Cham, 2021, pp. 1–7.
[52] J.E. Cavanaugh, A.A. Neath, The Akaike information criterion: Background, derivation, properties, application, interpretation, and refinements, Wiley Interdiscip. Rev. Comput. Stat. 11 (3) (2019) e1460.
[53] J. Ansary, A.K. Chaurasiya, K.B. Huq, Formulation and evaluation of metformin HCl floating microspheres, Asian J. Med. Biol. Res. 1 (3) (2016) 396–405.
[54] C.S. Brazel, N.A. Peppas, Modeling of drug release from swellable polymers, Eur. J. Pharm. Biopharm. 49 (1) (2000) 47–58.
[55] H. Vogelpoel, et al., Biowaiver monographs for immediate release solid oral dosage forms based on biopharmaceutics classification system (BCS) literature data: Verapamil hydrochloride, propranolol hydrochloride, and atenolol, J. Pharm. Sci. 93 (8) (2004) 1945–1956.
[56] Guideline on quality of oral modified release products, 2014.

[57] R.K. Verbeeck, et al., Biowaiver monographs for immediate-release solid oral dosage forms: Enalapril, J. Pharm. Sci. 106 (8) (2017) 1933–1943.
[58] A. Khan, et al., Enhancement of dissolution rate of class II drugs (Hydrochlorothiazide); a comparative study of the two novel approaches; solid dispersion and liqui-solid techniques, Saudi Pharm. J. 23 (6) (2015) 650–657.
[59] E.M. Agency, Reflection Paper on the Dissolution Specification for Generic Solid Oral Immediate Release Products with Systemic Action, European Medicines Agency Amsterdam, The Netherlands, 2017.